Am J Physiol Cell Physiol 319: C541–C551, 2020.
First published July 22, 2020; doi:10.1152/ajpcell.00233.2020.

RESEARCH ARTICLE

Regulation of Lin28a-miRNA *let-7b-5p* pathway in skeletal muscle cells by peroxisome proliferator-activated receptor delta

Hygor N. Araujo,[1] Tanes I. Lima,[1] Dimitrius Santiago P. S. F. Guimarães,[1] Andre G. Oliveira,[1] Bianca C. Favero-Santos,[1] Renato C. S. Branco,[1] Rafaela Mariano da Silva Araújo,[1] Alvaro F. B. Dantas,[1] Alex Castro,[3] Mara Patrícia T. Chacon-Mikahil,[3] Elaine Minatel,[2] Murilo V. Geraldo,[2] Everardo Magalhães Carneiro,[1] Alice C. Rodrigues,[4] Vihang A. Narkar,[5] and Leonardo R. Silveira[1]

[1]*Obesity and Comorbidities Research Center (OCRC), Campinas, Brazil;* [2]*Department of Structural and Functional Biology, Institute of Biology, University of Campinas (UNICAMP), Campinas, Brazil;* [3]*Laboratory of Exercise Physiology, School of Physical Education, University of Campinas, Campinas, Brazil;* [4]*Department of Pharmacology, University of Sao Paulo, Sao Paulo, Brazil; and* [5]*University of Texas Health McGovern Medical School, Institute of Molecular Medicine, Houston, Texas*

Submitted 26 May 2020; accepted in final form 10 July 2020

Araujo HN, Lima TI, Guimarães DS, Oliveira AG, Favero-Santos BC, Branco RC, da Silva Araújo RM, Dantas AF, Castro A, Chacon-Mikahil MP, Minatel E, Geraldo MV, Carneiro EM, Rodrigues AC, Narkar VA, Silveira LR. Regulation of Lin28a-miRNA *let-7b-5p* pathway in skeletal muscle cells by peroxisome proliferator-activated receptor delta. *Am J Physiol Cell Physiol* 319: C541–C551, 2020. First published July 22, 2020; doi:10.1152/ajpcell.00233.2020.—Lin28a/miRNA *let-7b-5p* pathway has emerged as a key regulators of energy homeostasis in the skeletal muscle. However, the mechanism through which this pathway is regulated in the skeletal muscle has remained unclear. We have found that 8 wk of aerobic training (Tr) markedly decreased *let-7b-5p* expression in murine skeletal muscle, whereas high-fat diet (Hfd) increased its expression. Conversely, Lin28a expression, a well-known inhibitor of *let-7b-5p*, was induced by Tr and decreased by Hfd. Similarly, in human muscle biopsies, Tr increased LIN28 expression and decreased *let-7b-5p* expression. Bioinformatics analysis of LIN28a DNA sequence revealed that its enrichment in peroxisome proliferator-activated receptor delta (PPARδ) binding sites, which is a well-known metabolic regulator of exercise. Treatment of primary mouse skeletal muscle cells or C2C12 cells with PPARδ activators GW501516 and AICAR increased Lin28a expression. Lin28a and *let-7b-5p* expression was also regulated by PPARδ coregulators. While PPARγ coactivator-1α (PGC1α) increased Lin28a expression, corepressor NCoR1 decreased its expression. Furthermore, PGC1α markedly reduced the *let-7b-5p* expression. PGC1α-mediated induction of Lin28a expression was blocked by the PPARδ inhibitor GSK0660. In agreement, Lin28a expression was downregulated in PPARδ knocked-down cells leading to increased *let-7b-5p* expression. Finally, we show that modulation of the Lin28a-*let-7b-5p* pathway in muscle cells leads to changes in mitochondrial metabolism in PGC1α dependent fashion. In summary, we demonstrate that Lin28a-*let-7b-5p* is a direct target of PPARδ in the skeletal muscle, where it impacts mitochondrial respiration.

let-7b; Lin28a; PPARδ; skeletal muscle cells

INTRODUCTION

According to the World Health Organization, more than 340 million people worldwide are suffering from metabolic diseases, which is estimated to further increase due to an inactive lifestyle and unhealthy diet. Mitochondrial dysfunction in peripheral tissues is central to the development of metabolic diseases including obesity, type 2 diabetes, and insulin resistance (1, 2, 30). Identification of the underlying cause of mitochondrial dysfunction is crucial for preventing the progression of metabolic diseases. The molecular control of mitochondrial function and biogenesis represents a central aspect of mammalian physiology, and defects in the integrity of this system cause severe perturbations to cellular homeostasis (14, 19). There is evidence that mitochondrial dysfunction is also correlated with increased reactive oxygen species (ROS) production triggering inflammation, which in turn impairs fatty acid and glucose metabolism (30). The mitochondrial function and biogenesis processes are molecularly regulated by a battery of transcription factors including nuclear receptors such as peroxisome proliferator-activated receptor delta (PPARδ) (19, 31). Another level of regulation is through microRNAs, which are described as small noncoding RNA molecules that disrupt posttranscriptional processes impairing protein translation (6, 8). Studies have demonstrated that physical exercise, a well-known stimulator of the mitochondrial function and biogenesis processes, induces changes in the miRNA levels (29). Moreover, miRNAs have been reported to play a role in numerous metabolic diseases, as its expression is substantially modified in mitochondrial dysfunction (28). In this context, miRNAs are promising candidates for regulating mitochondrial function and biogenesis in the skeletal muscle.

The miRNA *Let-7* was initially shown to control development in *Caenorhabditis elegans* (27). In fact, the *let-7* family is known for the antioncogenic role as they repress the translation of oncogenes and cell cycle regulators (12, 17). The miRNA *let-7* family was also demonstrated to exert a prominent role in regulating various biological functions, including metabolism (4, 9). Of note, whole body and pancreas-specific overexpression of miRNA *let-7* resulted in impaired glucose tolerance and reduced fat mass and body weight. On the other hand, knockdown of *let-7* in obese mice prevented these effects by improving insulin sensitivity in both liver and skeletal muscles indicating that *let-7* has a pivotal role in glucose metabolism (37). Although the mechanism is still unknown,

Correspondence: L. R. Silveira (leors@unicamp.br); V. A. Narkar (vihang.a.narkar@uth.tmc.edu).

these effects were in part mediated by inhibition of the insulin receptor substrate (IRS)/Akt insulin pathway in tissues such as muscle and liver.

By being conserved and widely expressed, the *let-7* expression is well regulated in different tissues (9, 37). The RNA-binding proteins Lin28a and Lin28b are important regulators of *let-7* expression by repressing its maturation process (11). Mice overexpressing Lin28a/b were protected against obesity exhibiting enhanced glucose tolerance. In contrast, knockout of Lin28a in skeletal muscle or overexpression of let-7 resulted in insulin resistance and impaired glucose tolerance indicating that the *let-7* induction negatively regulates mitochondrial metabolism (37). However, little is known about the molecular regulation of the Lin28/*let-7* axis. In skeletal muscle cells, PPARγ coactivator-1α (PGC1α)/PPARδ axis is a central regulator of mitochondrial homeostasis (25, 26). Using bioinformatics analysis, we identified several PPARδ binding sites throughout the Lin28a DNA sequence raising the possibility that *let-7b-5p,* a 5′-complementary sequence of hairpin *let-7b-3p*, is regulated by PPARδ in a Lin28a-dependent mechanism in skeletal muscle cells. Based on the therapeutic potential of miRNAs in pathologies related to metabolic diseases like obesity, diabetes, and cancer, it is essential to establish a clear understanding of the pathway involved in the control of *let-7b* expression. Here we have examined the role of nuclear receptor PPARδ and its coactivator PGC-1α in the regulation of Lin28a-*let-7b-5p* pathway in the skeletal muscle cells.

METHODS

miRNA/mRNA Interaction

MIRWALK 2.0 (http://zmf.umm.uni-heidelberg.de/apps/zmf/mirwalk2/custom.html) was used to perform bioinformatics analysis and interaction prediction between the miRNA *let-7b-5p* and mitochondrial biogenesis genes. Only genes predicted in at least 5 of the 12 prediction algorithms used by MIRWALK 2.0 were selected. After processing of the data, the PGC1α and PGC1β genes were chosen as study targets. The 3′-untranslated region (UTR) of PGC1α was cloned into the plasmid pmiRGlo (Promega, Fitchburg, WI) using 20 units of the enzymes XbaI and XhoI (NEB, Ipswich, MA). HEK293T cells were cotransfected with the reporter and transcription factor plasmids, and the luciferase activity was measured using the Dual-Glo luciferase assay system (Promega, Fitchburg, WI) according to the company protocol.

Ethical Procedures

All experiments in animals were approved by the Ethics Commission on Animal Use of the State University of Campinas–CEUA/UNICAMP with Protocol No. 4694-1/2017. The experiments in human tissue were approved by Unicamp Research Ethics Committee, registered under the number CAAE: 52997216.8.0000.5404, April 2016.

Experimental Procedures

Animal procedures. Male 4-wk-old C57BL/6Junib mice were kept in cages (4 animals/cage) at 21 ± 1°C in a 12-h light-dark cycle. Throughout the protocol, the animals had free access to water, standard diet (Nuvilab-CR1, Brazil), or high-fat diet (Prag Solution, Brazil). The animals were separated into three groups: control fed with a standard diet (Ct), physically trained fed with a standard diet (Tr), and fed with a high-fat diet (Hfd). Before the beginning of the physical training, all animals were submitted for 5 days of adaptation at a speed of 8 cm/s for 10 min. After adaptation, all animals performed the maximum speed test to determine the intensity of physical training (15). The test was started by 8-min warm up at a speed of 15 cm/s. At the end of the warm-up, the speed was increased by 5 cm/s every minute until the exhaustion and voluntary abandonment of the animal. The physical training protocol was performed only by group Tr for 1 h every day, 5 days per week during 8 wk, on a treadmill inclined to 25° and speed corresponding to 70% of the maximum speed obtained in the test. After 8 wk of aerobic exercise training, the animals were euthanized by deepening anesthetic using ketamine (300 mg/kg) and xylazine (30 mg/kg) followed by cervical dislocation, and the soleus muscles were collected and stored at −80°C for further analysis.

Human procedures. Briefly, the training program was performed on cycle ergometers, 40 min per session, for 8 wk. Participants exercised at 70% heart rate reserve (HRR), 3 days a week in the first 4 wk and at 75% HRR, 4 days a week in the last 4 wk (5).

Human biopsy. Tissue biopsies of the dominant lower limb's vastus lateralis muscle were performed according to the procedure described above (32). Before the tissue's extraction, the area was shaved and cleaned. A small area over the selected region was anesthetized with xylocaine (2%), injected subcutaneously. Then, a small incision (~5 mm) was made up to the muscle fascia using a surgical scalpel. The biopsy needle was inserted into the muscle (~3 cm) to obtain the sample. After extraction, all samples were cleaned (free of blood and excess connective tissue), aliquoted, immediately frozen in liquid nitrogen, and stored at −80°C for further analysis.

Culture of primary mouse skeletal muscle cells. Male C57BL/6Junib mice with 28-days-old were euthanized after ketamine (300 mg/kg) and xylazine (30 mg/kg) anesthesia followed by cervical dislocation. The hindlimb muscles were extracted in Dulbecco's phosphate-buffered saline (DPBS) containing glucose (1%) and penicillin (1%). The muscle tissues were minced and digested in Dulbecco's modified Eagle's medium (DMEM) containing collagenase type II (22 mg) and penicillin (1%) using shaker at 37°C for 90 min. After this enzymatic digestion, the cells were centrifuged at 1,200 *g* and 4°C for 20 min. The prime growth medium (PGM) was carefully removed, and a fresh DMEM containing collagenase type II (18 mg), trypsin (2.5%), DNAse I (0.1%), and penicillin (1%) and was incubated in a shaker at 37°C for 30 min. The trypsin was neutralized with PGM containing horse serum (10%), fetal bovine serum (10%), L-glutamine (2 mM), and penicillin (1%). The suspension was centrifuged at 1,200 *g* and 4°C for 20 min. Fresh PGM was added to the cell pellet, and the cell suspension was filtered through a 70-μM filter. The cells were seeded in dishes covered with Matrigel (0.1%) at a density of 2×10^5 cells/well and cultured at 37°C with 5% CO_2. After 48 h, PGM was replaced by fusion medium (FM) containing horse serum (10%) and L-glutamine (2 mM) until cell differentiation.

Culture of C2C12 cells. The C2C12 cells were purchased from ATCC. C2C12 cells were plated at a density of 2×10^5 cells/well in six-well plates. The maintenance medium used was DMEM medium containing fetal bovine serum (10%). The differentiation was realized in cells at 70% confluency switched to DMEM containing 2% horse serum for 5 days to induce differentiation. The experiments were performed after this period.

HEK 293T cells. Human embryonic kidney (HEK) 293T cells were purchased from ATCC. HEK 293T cells were plated at a density of 5×10^4 cells/well in DMEM medium containing fetal bovine serum (10%).

Cellular Transfection

Transfection of PGC1α. Differentiated primary mouse skeletal muscle cells seeded in a six-well dish were transfected in 1 mL of Opti-MEM medium containing 7.5 μL of LipofectamineTM 3000 (Life Technologies) and 4 μL of p3000 reagent and 2 μg of either pCDNA 3.1 PGC1α plasmid (Addgene no. 4551) or pCDNA3.1 empty vector (Addgene no. 128434) for a 48-h period. After the first

24 h, DMEM containing horse serum (10%) and L-glutamine (2 mM) was added and maintained for an additional 24 h.

Transfection of let-7b-5p mimic or inhibitor. Differentiated primary mouse skeletal muscle cells were plated in a six-well dish and transfected in 1 mL OPTIMEM medium containing 9 μL of Lipofectamine RNAiMAX (Life Technologies) and 100 nM of mimic or *let-7b-5p* inhibitor (ThermoFisher) during 48 h. After the first 24 h, DMEM containing horse serum (10%) and L-glutamine (2 mM) was added and maintained for an additional 24-h period. Scrambled interfering RNAs were used as control (negative control-ThermoFisher) was used.

Transfection of PGC1α and NCoR1. MEF cells were plated in a six-well dish and transfected in 1 mL of Opti-MEM medium containing Lipofectamine 3000 (Life Technologies), 2 μL of p3000 reagent, and 1 μg of either PGC1α (Addgene no. 4551) or NCoR1 plasmid (gift from Mitchell Lazar laboratory) for 48 h. After the first 24 h, 1 mL of DMEM medium containing fetal bovine serum (10%) was added and maintained for an additional 24-h period. Empty pCDNA3.1 plasmid (Addgene no. 128434) was used as control.

Drug treatments. To induce PPARδ, differentiated C2C12 or primary mouse skeletal muscle cells cultured in six-well dishes were exposed to the AMPK activator AICAR (250 μM) (Sigma-Aldrich, St. Louis, MO) during a period of 1, 3, or 6 h. Nuclease-free water (Sigma-Aldrich, St. Louis, MO) was used as the vehicle. In addition, either primary mouse skeletal muscle cells or C2C12 cells were exposed to the PPARδ agonist GW501516 (100 nM) (Sigma-Aldrich, St. Louis, MO). While the treatment in primary mouse skeletal muscle cells was during a period of 1, 3, or 6 h, the treatment in C2C12 was during a period of 1, 6, 12 or 24 h. The primary mouse skeletal muscle cells were also exposed to the PPARδ antagonist GSK 0660 (5 μM) (Cayman, Ann Arbor, MI) during a period of 24 or 36 h. DMSO (Sigma-Aldrich, St. Louis, MO) was used as the vehicle. Both vehicle and drug treatments in C2C12 were performed in DMEM containing horse serum (2%), while in primary mouse skeletal muscle cells the treatment was performed in FM medium containing horse serum (10%).

Luciferase Assay

3′-UTR PGC1α. Luciferase assay was performed on 24-well plates using HEK293T cells. Cells at 80% confluence were transfected in 0.5 mL of OPTI-MEM medium, 1.5 μL of Lipofectamine 3000 (Life Technologies, Carlsbad, CA); 1 μg of pmirGLO plasmid (Promega) containing 3′-UTR sequence of PGC1α; 20 nM of either scramble, mimic, or inhibitor of *let-7b-5p* (ThermoFisher); and 2 μL of p3000 reagent. After 24 h, transfected cells were lysed with 100 μL of 1× passive lysis buffer (Promega), and luciferase activity was measured in 20 μL of lysate in a 96-well white plate (costar) using the Dual-luciferase assay system (Promega) according to the manufacturer's instructions.

PPRE. Luciferase assay was performed on 24-well plates using HEK 293 cells. Cells at 80% confluence were transfected in 0.5 mL of OPTI-MEM medium containing 1.5 μL of Lipofectamine 3000 (Life Technologies, Carlsbad, CA); 0.05 μg of pRL-SV40 plasmid (E2231; Promega); 0.5 μg of PPRE X3-TK-luc plasmid (1015; Bruce Spiegelman; Addgene); 100 nM of either scramble, mimic, or inhibitor of *let-7b-5p* (ThermoFisher); and 0.5 μL of p3000 reagent. After 24 h, transfected cells were lysed with 100 μL of 1× passive lysis buffer (Promega), and luciferase activity measured in 20 μL of lysate in a 96-well white plate (Costar) using the Dual-luciferase assay system (Promega) according to the manufacturer's instructions.

Western blotting. Primary mouse myotube samples were homogenized in RIPA buffer (50 mM Tris·HCl, pH 7.4, 150 mM NaCl, 1 mM EDTA, 1% Triton X-100, 1% sodium deoxycholate, and 1% sodium dodecyl sulfate) containing protease inhibitor cocktail (Roche cOmplete, Mini, EDTA-free Protease Inhibitor Cocktail) and phosphatase inhibitors (10 mM sodium orthovanadate, 10 mM sodium pyrophosphate, and 10 mM sodium fluoride). The samples were sonicated, vortexed, and incubated on ice for 30 min. The lysates were cleared by centrifugation at 18,000 *g* at 4°C for 20 min. The protein concentration of the supernatant was determined by Pierce assay, and 40 μg of protein were loaded into SDS-PAGE gels. The proteins were transferred to nitrocellulose membrane and blocked at room temperature for 1 h with 5% skim milk in TBS-T buffer (0.02 M Tris·HCl, 0.16 M NaCl, and 0.1% Tween-20, pH 7.4). The membrane was washed three times with TBS-T and incubated overnight with the primary antibodies: β-actin (Santa Cruz no. SC81178), β-tubulin (Santa Cruz no. SC5274), vinculin (Cell Signaling no. 4650), Lin28a (Abcam ab155542), PPARδ (Invitrogen no. PA1-823A), and PGC1α (Calbiochem np. mAb4C1.3). The membrane was washed three times for 10 min with TBS-T and incubated with horseradish peroxidase (HRP)-conjugated secondary antibody (1:10,000) in blocking buffer for 1 h. After incubation with secondary antibodies, the membranes were washed three times in TBS-T solution. The images were obtained using Amersham Imager 600 (GE healthcare Life Sciences).

RNA extraction. RNA was extracted from differentiated primary mouse skeletal muscle cells, C2C12 cells, and MEF cells (2×10^6 cells) using 1 mL TRIzol (ThermoFisher) according to the manufacturer's instruction and RNA quantified by NanoDrop spectrophotometer (ThermoFisher). The quality of RNA extraction was measured by 260/280 and 260/230 ratio. All samples that presented values lower than 1.6 to both ratio were not used to cDNA synthesis.

Reverse transcription reaction for mRNA. Synthesis of complementary DNA was performed from total RNA (2 μg) using the High Capacity cDNA Reverse Transcription Kit (ThermoFisher) according to the manufacturer's instruction.

Reverse transcriptase-quantitative PCR reaction for mRNA. Gene expression was quantified by real-time PCR using Fast Real-Time PCR System (Applied Biosystems). The reactions were carried out in a mixture (10 μL) containing Invitrogen Fast SYBR Green Master Mix (5 μL), primers sequences (0.3 μM), sample cDNA (50 nM), and DEPC water (here volume needed to complete 10 μL). The cycle conditions used were 95°C for 20 s, 40 cycles at 95°C for 3 s and 60°C for 30 s, followed by melting curve at 95°C for 15 s, 60°C for 60 s, 95°C for 15 s and 60°C for 15 s. The relative expression of mRNAs was determined using the $2^{-\Delta\Delta Ct}$ method (20). TBP and RPL39 were used as housekeeping genes. The primer sequences were as follows: PDK4, forward: GGATTACTGACCGCCTCTTTAG; reverse: GTAACCAAAACCAGCCAAAGG; PGC1α, forward: CCCTGCCATTGTTAAGACC; reverse: TGCTGCTGTTCCTGTTTTC; NCOR1, forward: CTGGTCTTTCAGCCACCATT; reverse: CCTTCATTGGATCCTCCATC; LIN28a, forward: TGGTGGTGTGTTCTGTATTGG; reverse: GTAGCACCTGTCTCCTTTGGAT; TBP, forward: GTTGGGCTTCCCAGCTAAGT; reverse CACAAGGCCTTCCAGCCTTA; and RPL39, forward: CAAAATCGCCCTATTCCTCA; reverse: AGACCCAGCTTCGTTCTCCT.

Reverse transcription reaction for miRNA. Total RNA was extracted from either primary mouse myotubes (20 ng) or human quadriceps muscles (20 ng). Synthesis of complementary DNA (cDNA) was performed using the TaqMan Micro-RNA Reverse Transcription (Applied Biosystems) kit containing primers stem-loop for *let-7b-5p*, hsa-RNU24a, and mmu-SNO-202 obtained from TaqMan MicroRNA Assays (ThermoFisher), and all procedures were done according to the manufacturer's instructions.

Reverse transcription-quantitative PCR reaction for miRNA. For cDNA synthesis, the total RNA was extracted from either primary mouse skeletal muscle cells (12.5 ng), mice soleus skeletal muscle (5 ng), or human quadriceps muscle (5 ng). PCR reactions used TaqMan Universal Master Mix (Applied Biosystems) containing oligonucleotides and probes TaqMan MicroRNA Assay (Applied Biosystems). All the reactions were run on the 7500 Fast Real-Time PCR System (Applied Biosystems), and the relative expression of miRNAs was determined using $2^{-\Delta\Delta Ct}$ method (20).

Oxygen consumption. Primary mouse skeletal muscle cells were seeded in 24-well Seahorse plates at a density of 10^5 cells/well and differentiated to myotubes. Cells were then transfected with either scramble, mimic, or inhibitor *let-7b-5p* 48 h before the assays. Following incubation with respiration medium (Krebs buffer pH 7.4 supplemented with 4 mM L-glutamine, 1 mM sodium pyruvate, and 5 mM glucose) at 37°C for 1 h without CO_2, oxygen consumption rate (OCR) was measured using a Seahorse respirometer (XF24, Agilent Technologies) according to the manufacturer's instructions. The following drugs were injected sequentially after basal OCR measurement: 1 μM of oligomycin to inhibit ATP synthase, 2 μM of the protonophore carbonyl cyanide m-chlorophenyl hydrazone (CCCP) to uncouple mitochondrial electron transport from ATP synthesis, and 1 μM of rotenone/antimycin to block mitochondrial respiration. ATP-linked OCR was calculated by subtracting the OCR after oligomycin addition from basal OCR. Spare capacity was determined by subtracting basal from the CCCP-induced OCR. The nonmitochondrial OCRs were subtracted from all absolute values. All Seahorse measurements were normalized by protein quantified by Pierce assay.

Chromatin immunoprecipitation-sequencing analysis. PPARδ chromatin immunoprecipitation-sequencing (ChIP-seq) data from C2C12 myotubes treated with GW501516 (SRR4011745) or control (SRR4011744) were extracted from the European Bioinformatics Institute (EBI) database and processed with the Galaxy online platform (10, 16). After verification of the quality of the extracted reads with Fastqc, they were aligned against the mouse genome (mm9) using Bowtie for Illumina with default settings. The coverage ratio was calculated with bamCompare with a 25-bp tray and a pseudocount of 1. The coverage file generated was visualized using the University of California, Santa Cruz (UCSC) Genome Browser. The presented ChIP-seq data from MYOD1 and MYOG1 from the ENCODE project is available in the Genome Browser public tracks.

RESULTS

Aerobic Exercise Regulates Let-7b-5p Expression in a Lin28a-Dependent Manner

Since the *let-7b* family of microRNAs regulates mitochondrial function (9) we investigated whether aerobic exercise or diet-induced obesity affects skeletal muscle *let-7b-5p* expression in vivo. Aerobically trained mice (Tr) showed reduced expression of *let-7b-5p* in soleus muscle, whereas mice subjected to high-fat feeding (Hfd) had the opposite effect (Fig. 1*A*) suggesting that elevated mitochondrial functionality is reciprocally associated with low expression of *let-7b-5p*. As Lin28a regulates *let-7b-5p* expression (11), we further investigated whether aerobic exercise or diet-induced obesity could also change Lin28a expression in vivo. The expression of Lin28a was induced in skeletal muscle of mice subjected to aerobic training for 8 wk (Tr), whereas it was reduced after a high-fat diet (Hfd) treatment for the same period (Fig. 1, *B* and *C*). Similar findings were also observed in the vastus lateralis muscle of humans as demonstrated by increased expression of LIN28a after aerobic training (Fig. 1, *E* and *F*). The *let-7b-5p* expression was also reduced after 8 wk of aerobic training (AT) in human skeletal muscle demonstrating that aerobic training represses *let-7b-5p* expression (Fig. 1*D*), an effect that seems to be associated with Lin28a induction.

PPARδ Regulates Lin28a Expression

The mitochondrial function is molecularly regulated by the activity of different transcription factors including nuclear

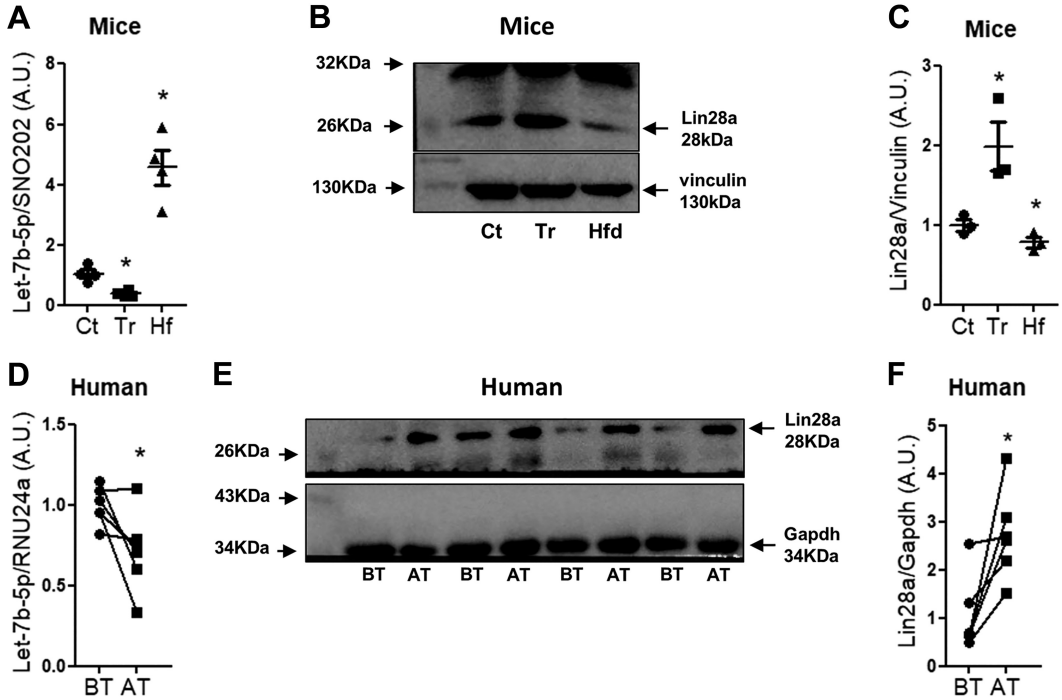

Fig. 1. Aerobic exercise regulates *let-7b-5p* expression in a Lin28a-dependent mechanism. *A*: expression of miRNA *let-7b-5p* in the soleus from control (Ct), physically trained (Tr), and fed high-fat diet (Hfd) mice ($n = 4$). A.U., arbitrary units. *B*: Lin28a protein expression in the soleus of different groups including control (Ct), physically trained (Tr), and fed high-fat diet (Hfd) mice ($n = 3$). *C*: densitometry analysis of Lin28a/vinculin. *D*: expression of *let-7b-5p* in vastus lateralis of humans before (BT) and after (AT) training ($n = 5$). *E*: Lin28a protein expression in vastus lateralis of humans before (BT) and after (AT) physical training ($n = 6$). *F*: densitometry analysis of Lin28a/GAPDH. Error bars represent SE. $^*P \leq 0.05$ compared with control. One-way ANOVA followed by Tukey posttest was used in mice experiments, whereas a paired Student's *t* test was used in human experiments.

receptor PPARδ in a PGC1α-dependent mechanism, and both these factors have been shown to have exercise mimetic effects in the skeletal muscle (22, 25). Therefore, we next investigated whether PPARδ is involved in the regulation of Lin28a and *let-7b-5p* in the skeletal muscle. Using public Chip-seq data from Fan and colleagues (7), we observed that PPARδ is largely enriched at 22, 32, and 42Kb LIN28a promoter position suggesting that PPARδ affects Lin28a transactivation (Fig. 2*A*). Lin28a has been described as a major regulator of *let-7b-5p* in different tissues including skeletal muscle (9, 37). We also observed that DNAse footprint showed different points overlapping with PPARδ enrichment indicating that the chromatin is decondensed by transcriptional machinery. Besides, myogenin was found to be largely enrichment at these DNA

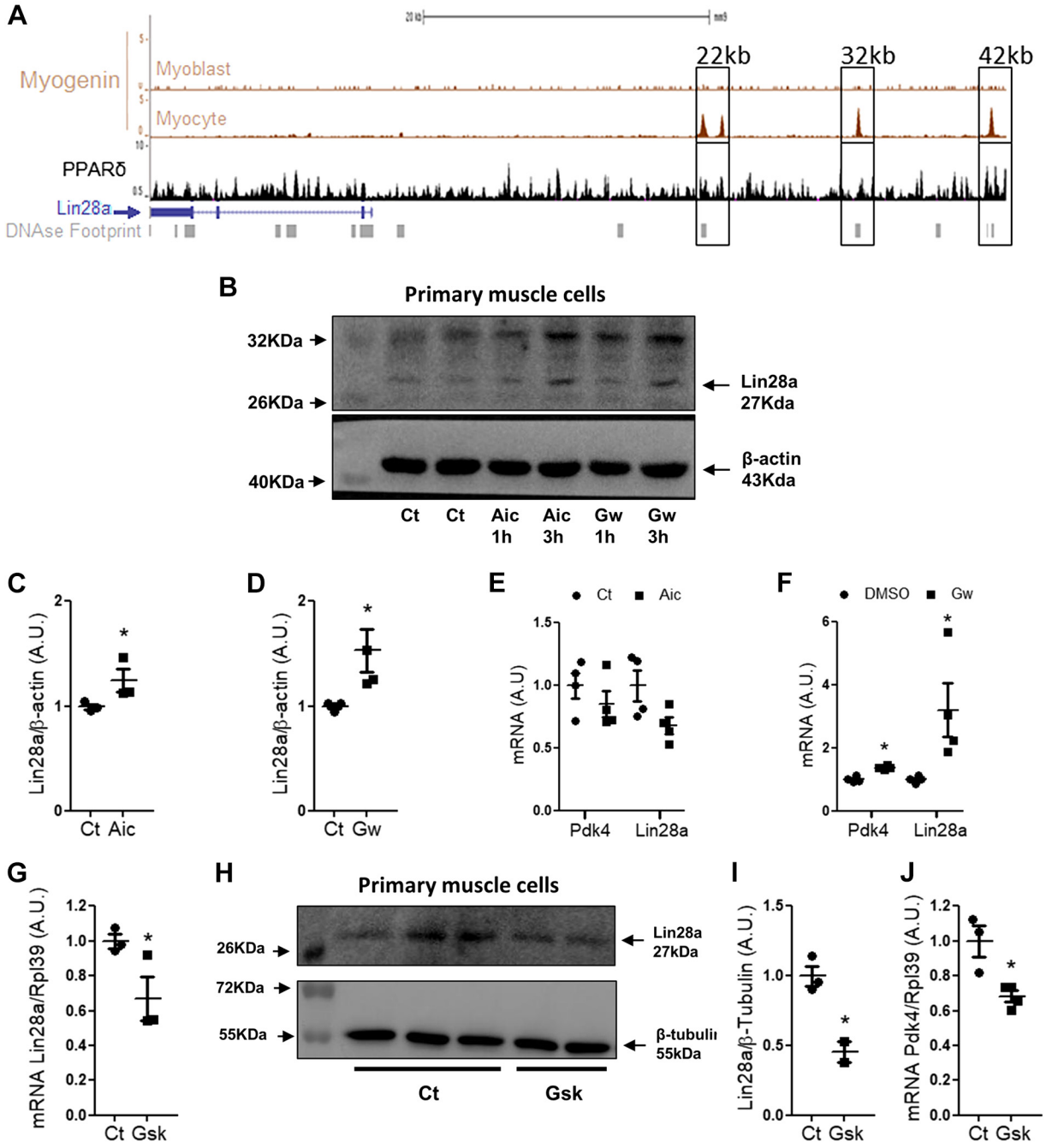

Fig. 2. Peroxisome proliferator-activated receptor delta (PPARδ) regulates Lin28a expression. *A*: chromatin immunoprecipitation-sequencing (ChIP-seq) analysis at the *LIN28a* promoter region in C2C12 cells treated with GW501516 or vehicle. *B*: expression of Lin28a protein in cultured murine skeletal muscle cells treated with either AICAR (Aic; 250 μM) or GW501516 (Gw; 100 nM) for 1 and 3 h, $n = 1$ from 3 independent experiments. *C* and *D*: densitometry analysis of Lin28a/actin protein at 3 h. Ct, control; A.U., arbitrary units. *E* and *F*: expression of genes *PDK4* and *LIN28a* in cultured mouse skeletal muscle cells treated with either AICAR (250 μM) or GW501516 (100 nM) for 3 h ($n = 4$). *G*: expression of *Lin28a* in cultured mouse skeletal muscle cells exposed to GSK0660 (Gsk; 5 μM) for 36 h ($n = 4$). *H*: LIN28a protein expression in cultured mouse skeletal muscle cells exposed GSK0660 (5 μM) for 36 h ($n = 2$–3). *I*: densitometry analysis of Lin28a/tubulin protein. *J*: expression of *PDK4* in cultured mouse skeletal muscle cells exposed GSK0660 (5 μM) for 36 h ($n = 4$). Means ± SE are shown. *$P \leq 0.05$ compared with control. An unpaired Student's *t* test was used for statistical analysis.

regions during C2C12 differentiation (Fig. 2*A*). Cellular differentiation is an expensive thermodynamic process in biological systems suggesting that LIN28a is associated with mitochondrial function in skeletal muscle cells. Primary mouse skeletal muscle cells exposed to different PPARδ activators including AICAR (250 μM) or GW501516 (100 nM) (22) had increased Lin28a content at 3 h after treatment (Fig. 2, *B–D*), and this effect was consistent with the increased transcription of Lin28a after GW501516 treatment but not with AICAR (Fig. 2, *E* and *F*). To confirm PPARδ activation, *PDK4*, a well-known downstream target of PPARδ was evaluated as control (13) (Fig. 2, *E* and *F*). Similar findings were also obtained in primary skeletal mouse cells treated with either AICAR, caffeine, GW, or isoproterenol during a period of 6 h, and this effect was associated with increased Lin28a content (Supplemental Fig. S1*A*; see https://doi.org/10.6084/m9.figshare.12624266.v2). The GW501516 effect was also evaluated on *Lin28a* and *PDK4* mRNA levels, and we observed that *Lin28a* transcription was upregulated from 12 up to 24 h, whereas *PDK4* from 3 up to 24 h (Supplemental Fig. S1, *B* and *C*). In order, to confirm these findings C2C12 cells were exposed to GW501516 (100 nM) for 12 h, and the Lin28a content was markedly increased (Supplemental Fig. S1, *D* and *E*).

Next, we exposed cultured mouse skeletal muscle cells to PPARδ antagonist GSK0660 (5 μM) for 36 h. Under such conditions, transcription of *LIN28a* was reduced and this effect was accompanied by reduced protein level (Fig. 2, *G–I*). These findings suggest that Lin28a regulates *let-7* via a PPARδ-dependent mechanism. *PDK4* expression was also markedly reduced under GSK0660 treatment confirming an inhibitory effect of GSK0660 on PPARδ activity (Fig. 2*J*).

Let-7b Is Regulated by LIN28a in a PPARδ-Dependent Mechanism

Transcription of mitochondrial genes regulated by PPARδ depends on its binding to peroxisome proliferator response element sequence at mitochondrial gene promoters (23, 24, 35). This regulatory process allows the cells to promptly regulate the expression of mitochondrial genes in response to cellular stress as observed during aerobic exercise. Thus, to induce PPARδ transactivation, we overexpressed the PPARδ coactivator PGC1α in cultured murine myoblasts as indicated by protein level and mRNA (Fig. 3, *A*, *B*, and *D*). Under such conditions, both protein (Fig. 3, *A* and *C*) and mRNA (Fig. 3*E*) levels of LIN28a were markedly increased and this effect was associated with the upregulation of *PDK4* used as positive control (Fig. 3*F*). Of note, *let-7b-5p* was reduced in PGC1α-overexpressing cells indicating that increased PPARδ transactivation is associated with *let-7b-5p* regulation (Fig. 3*G*). Similar findings were also obtained when PPAR coregulators were overexpressed in MEF cells. While PGC1α markedly increased Lin28a, NCoR1 overexpression had the opposite effect, decreasing the Lin28a expression (Supplemental Fig. S1, *F* and *G*). The NCoR1 overexpression was also observed to decrease both *PDK4* and *Lin28a* transcription levels (Supplemental Fig. S1*H*).

To confirm the role of PPARδ in PGC1α -mediated LIN28a expression, cultured mouse skeletal muscle cells were exposed to the PPARδ antagonist GSK0660, followed by PGC1α overexpressed (Fig. 3*H*). The PPARδ transactivation was markedly inhibited as indicated by *PDK4* expression (Fig. 3*I*), and this effect abolished the LIN28a expression (Fig. 3, *J–L*). Similarly, knockdown of PPARδ (43% vs. scramble) decreased *PDK4* expression (Fig. 3, *M* and *N*), and this effect was associated with reduced LIN28a level (Fig. 3, *M* and *O*). Interestingly, *let-7b-5p* expression was markedly upregulated indicating that PPARδ activation is critical for controlling the LIN28a and *let-7b-5p* levels in skeletal muscle cells (Fig. 3*P*). To confirm these findings, we also measured PPARδ content in skeletal muscle of aerobically trained mice. After 8 wk of training, the skeletal muscles exhibited increased PPARδ content (Fig. 3*Q*). Consistent with elevated PPARδ expression, *PDK4* transcription was also increased indicating low pyruvate dehydrogenase activity and increased lipid metabolism (Fig. 3*R*). In contrast, mice subjected to high-fat diets had reduced expression of PPARδ without a change in the *PDK4* transcription (Fig. 3, *Q–R*). As observed in mice, the expression of PPARδ was also increased in human vastus lateralis muscle after aerobic training (Fig. 3, *S* and *T*), further solidifying the idea that aerobic training induces PPARδ leading to low expression of *let-7b-5p* via a Lin28a-dependent mechanism. However, we did not observe any effect on the mitochondrial electron transport chain after 8 wk of aerobic training or Hfd treatment in mice (Supplemental Fig. S1, *L* and *O*). Nevertheless, the effect of aerobic exercise training mitochondrial electron transport chain protein expression was observed when the aerobic exercise training was performed for 10 wk (Supplemental Fig. S1, *M* and *P*). Similarly in humans, the mitochondrial electron transport chain protein expression was induced after 10 wk of aerobic exercise training (Supplemental Fig. S1, *N* and *Q*).

Fig. 3. *Let-7b* is regulated by LIN28a in a peroxisome proliferator-activated receptor delta (PPARδ)-dependent mechanism. *A*: content of LIN28a protein in cultured mouse skeletal muscle cells transfected with a vector containing the PPARγ coactivator-1α (PGC1α) DNA sequence or empty vector as control. The PGC1α content was also measured as internal control; $n = 4$ in 2 different experiments. *B* and *C*: densitometry analysis of PGC1α/tubulin and Lin28a/tubulin protein. A.U., arbitrary units. *D–G*: expression of genes PGC1α, *LIN28a*, *PDK4*, and miRNA *let-7b-5p* in cultured mice skeletal muscle cells transfected with PGC1α ($n = 4$). *H* and *I*: expression of *PGC1α* and *PDK4* in cultured mouse skeletal muscle cells transfected with PGC1α and exposed to PPARδ antagonist, GSK0660 (5 μM), for a period of 36 h ($n = 4$). *J*: Lin28a content in cultured mice skeletal muscle cells transfected with PGC1α and exposed to the PPARδ antagonist GSK0660 (5 μM) for a period of 36 h ($n = 3$). *K*: densitometry analysis of Lin28a/vinculin. *L*: transcription of *Lin28a* in cultured mouse skeletal muscle cells transfected with PGC1α and exposed to the PPARδ antagonist GSK0660 (5 μM) for a period of 36 h ($n = 3$). *M*: content of LIN28a protein in cultured mice skeletal muscle cells transfected with PPARδ siRNA (125 nM and 500 nM). The PPARδ content was also measured as internal control; $n = 2$ independent experiments. *N* and *P*: expression of *PDK4*, *LIN28a*, and miRNA *Let-7b-5p* ($n = 3$). *Q*: PPARδ protein expression in the *soleus* of different mice groups including control (Ct), physically trained (Tr), and fed high-fat diet (Hfd) ($n = 3$). *R*: *PDK4* mRNA levels in the soleus of mice ($n = 4$). *S*: PPARδ protein expression in vastus lateralis of humans before (BT) and after (AT) physical training ($n = 5$). *T*: densitometry analysis of PPARδ/GAPDH content in the vastus lateralis of humans. Error bars represent SE. $^*P \leq 0.05$ compared with control. One-way ANOVA followed by Tukey's posttest was used in mouse experiments, whereas a paired Student's *t* test was used in human experiments.

PPARδ Regulates Mitochondrial Function by Repressing the Let-7b-5p Expression in a PGC1α-Dependent Manner

It is known that PGC1α overexpression induces mitochondrial function and biogenesis (18, 34). We observed that transfection of cultured mouse skeletal muscle cells with the *let-7b-5p* inhibitor increased citrate synthase activity (Supplemental Fig. S1*I*) and this effect was associated with increased oxygen consumption rate (OCR) at basal state, increased ATP-linked OCR, spare capacity and proton leak (Fig. 4, *A–E*),

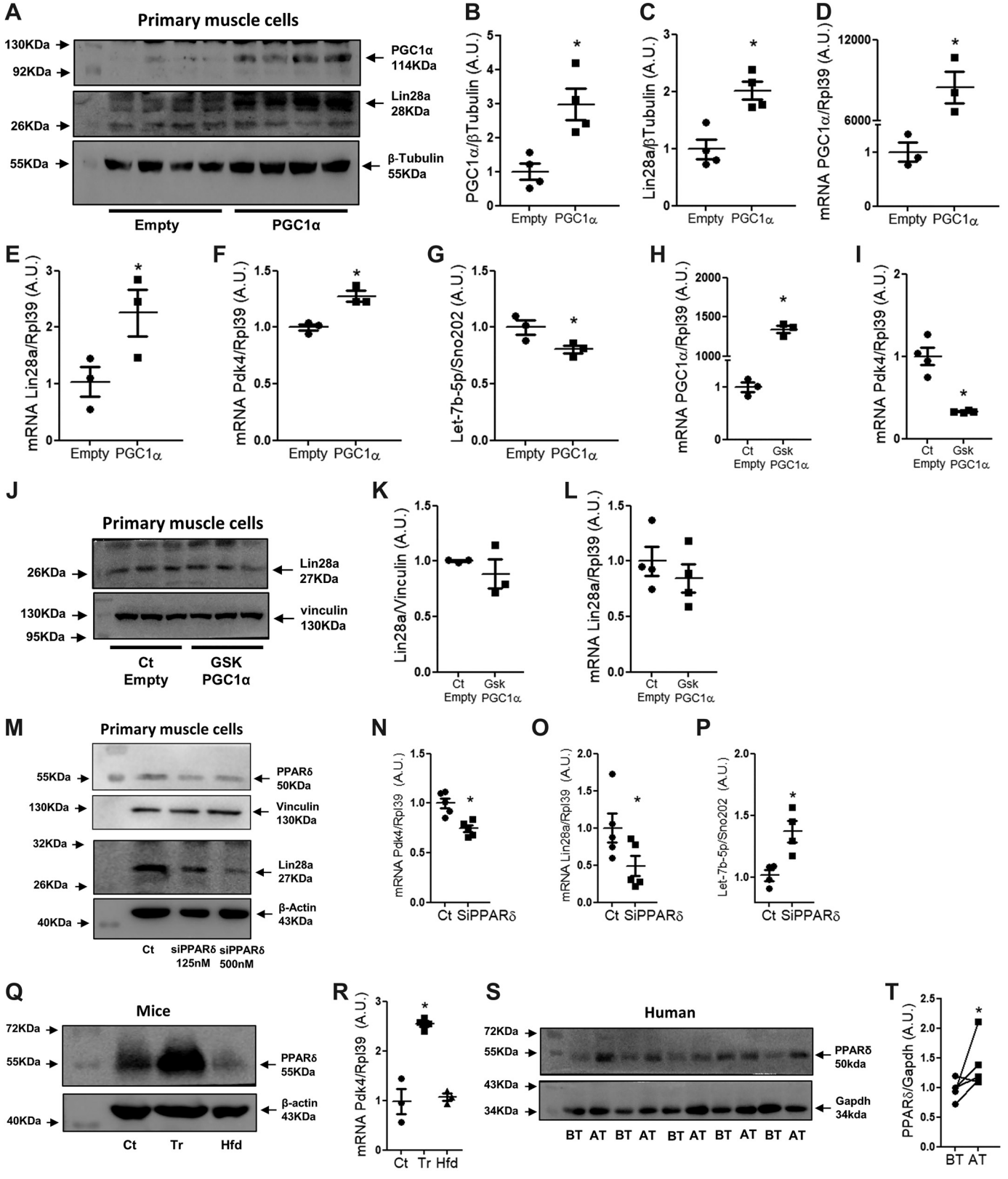

indicating that under low levels *let-7b-5p* can lead to increased mitochondrial function in skeletal muscle cells. Interestingly, knockdown of PGC1α abolished the *let-7b-5p* inhibitor effect on oxygen consumption, showing that the effect of the *let-7b-5p* inhibitor on mitochondrial respiration is regulated, at least in part, by a PGC1α-dependent mechanism (Fig. 4, *F–J*). In line with the above findings, HEK293T transfected with *let-7b-5p* inhibitor had a marked induction on PPRE activity (Supplemental Fig. S1*J*). Moreover, *let-7b-5p* expression was markedly reduced in brown adipose tissue from mice physically trained for 8 wk, a well-known condition associated with PGC1α induction (25, 26) (Supplemental Fig. S1*K*).

Let-7b-5p Targets the 3′-UTR Sequence of PGC1α mRNA

To understand how *let-7b-5p* regulates PGC1α mRNA, we explored the MIRWALK database and found that *let-7b-5p* targets 3′-UTR sequence of *PPARGC1α*, a central coactivator involved in mitochondrial biogenesis and function (Fig. 5*A*). Initially, the *let-7b-5p* expression was evaluated in cultured murine skeletal muscle cells under transfection of either *let-7b-5p* mimic or *let-7b-5p* inhibitor. Our findings showed that *let-7b-5p* mimics transfection markedly increased *let-7b-5p* expression, whereas transfection of *let-7b-5p* inhibitor markedly reduced *let-7b-5p* expression (Fig. 5*B*). Next, to confirm binding between *let-7b-5p* and 3′-UTR sequence of *PGC1α*, we cloned the predicted mRNA binding sequence into a luciferase reporter plasmid. HEK293 cells transfected with a mimic of *let-7b-5p* had reduced luciferase activity, whereas transfection with the inhibitor of *let-7b-5p* had the opposite effect indicating that 3′-UTR sequence of *PGC1α* is targeted to *let-7b-5p* (Fig. 5, *C* and *D*, respectively). Next, we measured the PGC1α protein level. When overexpressed, *let-7b-5p* reduced the expression of PGC1α (Fig. 5, *E* and *F*), while *let-7b-5p* inhibition led to an increased expression of PGC1α in cultured mouse skeletal muscle cells increasing the evidence that *let-7b-5p* binds to 3′-UTR sequence of *PGC1α* regulating its expression (Fig. 5, *G* and *H*).

Taken together, our findings demonstrate that aerobic training induces Lin28a in a PPARδ-dependent mechanism leading to low *let-7b-5p* expression and increase in cellular respiration in PGC1α-dependent fashion (Fig. 6).

DISCUSSION

The mitochondrial proteins are encoded by either nuclear or mitochondrial DNA in a synchronized process regulated by nuclear coregulators and transcriptional factors (19). Genetic evidence has linked mitochondrial dysfunction to low expression of peroxisome proliferator-activated receptor delta (PPARδ). PPARδ is a major transcription factor associated with mitochondrial function and biogenesis in skeletal muscle (26, 31). It is not surprising, therefore, that PPARδ activity is significantly reduced in skeletal muscle in diabetes

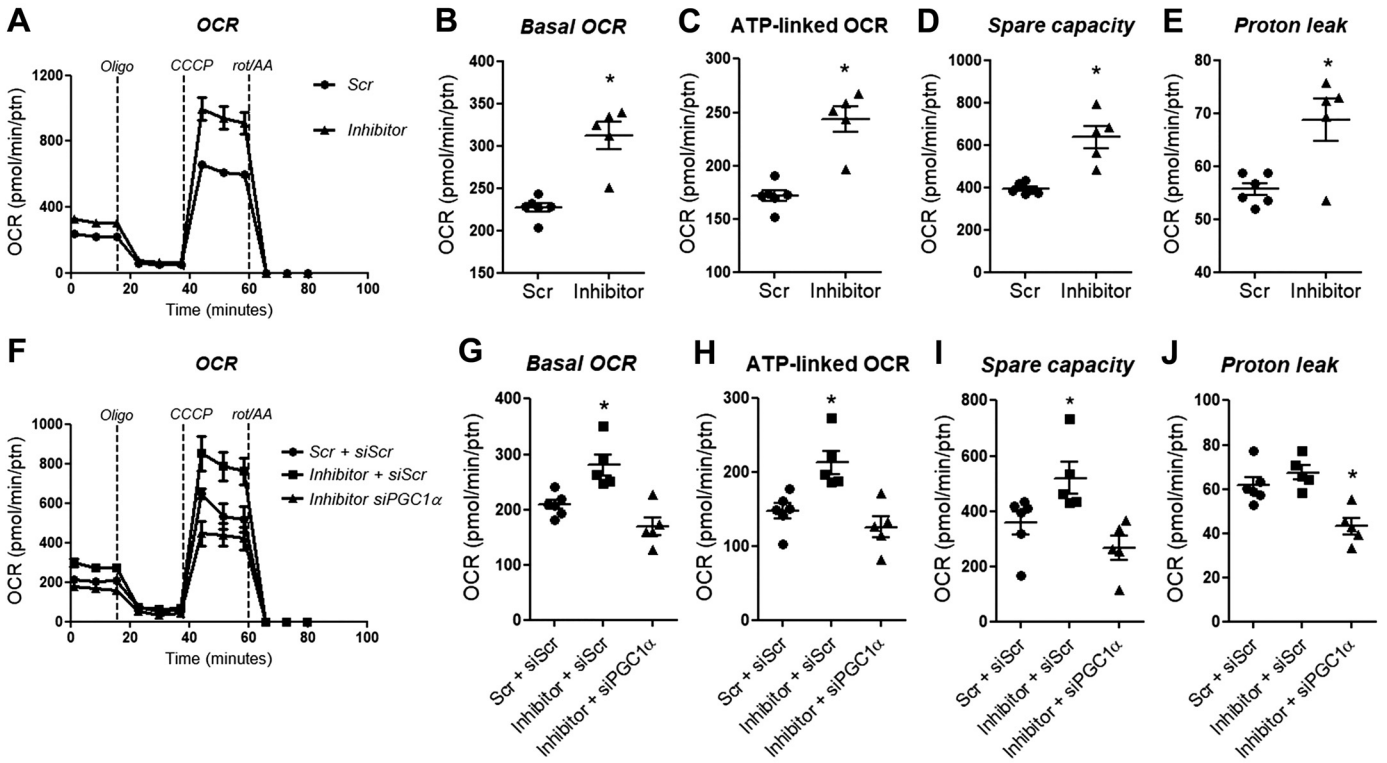

Fig. 4. Peroxisome proliferator-activated receptor (PPAR) regulates mitochondrial function by repressing the *let-7b-5p* expression in a PPARγ coactivator-1α (PGC1α)-dependent mechanism. *A*: oxygen consumption rate (OCR) of cultured mice skeletal muscle cells transfected with *let-7b-5p* inhibitor. Oligomycin (oligo; 1 μM) and CCCP (2 μM) were used for oxidative phosphorylation inhibition and mitochondrial uncoupling, respectively. *B–E*: basal OCR (*B*), ATP-linked oxygen consumption rate (OCR) (*C*), spare capacity (*D*), and proton leak (*E*) were evaluated ($n = 5$). *F*: OCR of cultured mice skeletal muscle cells cotransfected with either *let-7b-5p* inhibitor plus siPGC1α (100 nm). As a control, mice skeletal muscle cells were cotransfected with scramble of *let-7b-5p* inhibitor (Scr) plus scramble sequence of siPGC1α (siScr) ($n = 5$). *G–J*: basal OCR (*G*), ATP-linked OCR (*H*), spare capacity (*I*), and proton leak (*J*) were evaluated ($n = 5$). Scr, scramble; siScr, small interference scramble; siPGC1α, small interference PGC1α RNA sequence; rot/AA, rotenone/antimycin A. Error bars represent SE. $^*P \leq 0.05$, compared with control. One-way ANOVA was used for all experiments.

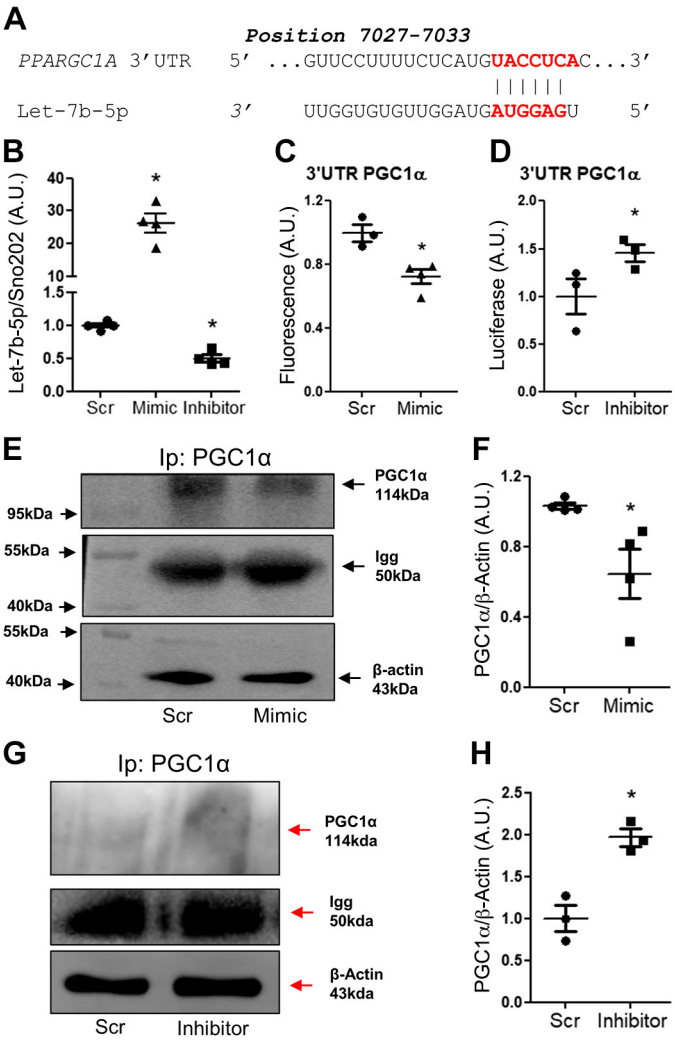

Fig. 5. *Let-7b*-5p targets the mRNA 3′-untranslated region (UTR) sequence of the peroxisome proliferator-activated receptor (PPAR)γ coactivator-1α (PGC1α). *A*: analysis of PGC1α 3′-UTR region by MIRWALK. *B*: expression of *let-7b-5p* in cultured mouse skeletal muscle cells transfected with either *let-7b-5p* mimic or *let-7b-5p* inhibitor ($n = 5$). A.U., arbitrary units. *C* and *D*: luciferase assay using a pmirGLO plasmid with PGC1α 3′-UTR cloned and transfected with either mimic (*C*) or inhibitor (*D*) of miRNA *let-7b-5p* in HEK 293, 2 independent experiments and ($n = 4$). *E* and *G*: PGC1α protein expression in cultured mouse skeletal muscle cells transfected with either mimic (*E*) or inhibitor (*G*) of *let-7b-5p*. Ip, immunoprecipitation. *F* and *H*: densitometry analysis. Western blotting was performed in 2 independent experiments ($n = 1$ for each experiment). Error bars represent SE. $^*P \leq 0.05$. Scr: Scramble; mimic, *Let-7b-5p*; inhibitor: inhibitory sequence of *let-7b*. $^*P \leq 0.05$ compared with control. Unpaired *t* test was used for statistical analysis.

(23, 25). PPARδ activity is highly regulated by hormones like epinephrine and thyroid hormone and also different kinases including AMPK, Sirt, PKA, Creb, MAPK, and Akt (2, 26, 25, 31). Another level of mitochondrial regulation occurs through microRNAs in a process disrupting posttranscriptional activity by impairing translation (3). Genetic dicer knockout that results in inhibition of miRNA processing provides convincing evidence that miRNAs are critical for different biological processes including mitochondrial metabolism (21). Here, we demonstrate that induction on PPARδ activity strongly decreases *let-7b-5p* expression in skeletal muscle cells via a Lin28a-dependent mechanism. Conversely, when PPARδ activity is suppressed, *let-7b-5p* expression is upregulated leading to impaired mitochondrial function. This finding, therefore, reveals a new mechanism in which mitochondrial function is regulated by *let-7b-5p* in a PPARδ/Lin28a-dependent manner.

It is noteworthy that the activation of PPAR isoforms has been implicated in the treatment of a number of metabolic diseases (33). Our findings show a substantial enrichment of PPARδ at *Lin28* promoter suggesting that PPARδ is a key regulator of Lin28a. Supporting this hypothesis, PPARδ levels were clearly associated with Lin28a expression when cultured mouse skeletal muscle cells were exposed to either GW501516 or AICAR, two well-known PPARδ activators (22). Lin28a/b expression in mice resulted in increased insulin sensitivity and resistance to diabetes, a phenotype typically associated with PPARδ activation and consequent induction of oxidative metabolism (36). Moreover, we found that the Lin28a level was upregulated in PGC1α overexpressing cells, and this effect was consistent with low *let-7b-5p* expression in these cells. Both knockdown of PPARδ and exposure of cultured primary mice skeletal muscle cells to GSK0660, a PPARδ antagonist, completely inhibited this effect solidifying the conclusion that *let-7b-5p* is regulated by PPARδ in a Lin28a-dependent mechanism. NCoR1, as well as PGC1α, was also observed to affect Lin28a expression in MEF cells. While PGC1α induced Lin28a expression, NCoR1 had the opposite effect, and this was consistent with a lower PPAR activity as indicated by PDK4 level (Supplemental Fig. S1, *F–H*). Zhu et al. (37) demonstrated that Lin28a/b has an important role in *let-7b* regulation and consequently on growth and glucose metabolism. In our study, the reduced expression of *let-7b* in the soleus muscle of mice after aerobic training was consistent with increased expression of Lin28a, whereas Hfd treatment had the opposite effect. Aerobically trained mice were also observed to exhibit increased PPARδ protein expression, while mice on high-fat diets had reduced expression of PPARδ, supporting the idea that PPARδ, at least in skeletal muscle cells, regulates mitochondrial function by a mechanism dependent of *let-7b*/Lin28a. It is widely accepted that aerobic training induces PGC1α expression in skeletal muscle (22). However, we failed to see any effect of Tr or Hfd treatment for 8 wk on proteins of mitochondrial electron transport chain in skeletal muscle of mice (Supplemental Fig. S1, *L* and *O*). This effect was apparent only when the aerobic training protocol was

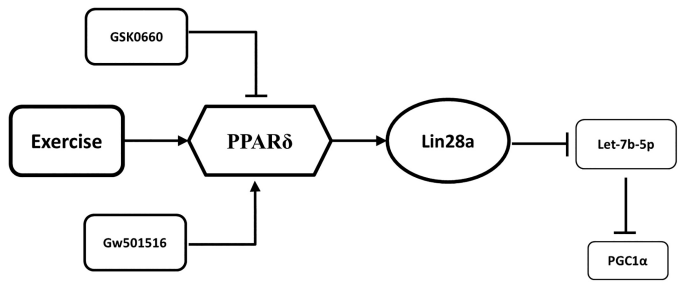

Fig. 6. Schematic model. Peroxisome proliferator-activated receptor delta (PPARδ) activity stimulated by either aerobic training or GW501516 induces Lin28a leading to a low *let-7b-5p* expression in skeletal muscle cells. In contrast, PPARδ inhibition by GSK0660 decreases Lin28a expression leading to upregulation of *let-7b-5p* expression and consequently reduced expression of PPARγ coactivator-1α (PGC1α).

extended to 10 wk (Supplemental Fig. S1, *M* and *P*), supporting the concept that mitochondrial function is not completely associated with mitochondrial biogenesis. Next, we addressed the question of whether this mechanism also occurs in humans. The PPARδ expression in human quadriceps muscle was markedly induced in response to 10 wk of aerobic exercise, and this effect was consistent with augmented Lin28a expression and lower expression of *let7b*, suggesting that Lin28a activity is necessary to prevent skeletal muscle against *let-7b* accumulation and consequently mitochondrial dysfunction. Of note, the content of mitochondrial electron transport chain proteins was markedly increased in human skeletal muscle after 10 wk of aerobic training (Supplemental Fig. S1, *N* and *Q*).

As *let-7b* was demonstrated to physically interact with *PGC1α* 3′-UTR mRNA sequence, we next investigated whether *let7-b* regulates PGC1α expression and consequently mitochondrial function in skeletal muscle cells. The inhibition of *let-7b-5p* increased PGC1α expression, and this effect was consistent with an increased mitochondrial function as indicated by analysis of cellular oxygen consumption in primary mouse cultured skeletal muscle cells. On the other hand, knockdown of PGC1α abolished the inhibitory effect of *let-7b* on mitochondrial respiration indicating that, at least in part, *let-7b-5p* regulates mitochondrial function in a PGC1α-dependent mechanism. Moreover, inhibition of *let-7b* in HEK cells marked induced PPRE activity suggesting increased activity of PGC1α/PPARδ complex. Similarly, in mice under a high-fat diet, *let7-b* antimir treatment resulted in increased lean and muscle mass suggesting increased oxidative phenotype (9). As mitochondrial stress is associated with low PGC1α expression and mitochondrial dysfunction (30), our findings point to a new mechanism of PGC1α regulation in the skeletal muscle cells.

In conclusion, our work identifies a previously unknown link between the classical PGC1α-PPARδ transcriptional pathway and Lin28a-*let-7b-5p* microRNA system that collectively pays a role in the regulation of mitochondrial biogenesis and cellular respiration in the skeletal muscle cells. The identified reciprocal role of PPARδ and *let-7b-5p* in both exercise-trained and diabetic skeletal muscle improves our understanding of metabolic regulation in skeletal muscle. Based on the therapeutic potential of miRNAs in pathologies related to the metabolic disease, these findings open new therapeutic strategies to prevent mitochondrial dysfunction and metabolic diseases in skeletal muscle cells in conjunction with PPARδ targeting.

ACKNOWLEDGMENTS

The authors thank Claudio C. Zoppi, Emerielle C. Vanzela, Fabiana Kuhne, and Tatiane R. Silveira for excellent technical assistance.

GRANTS

This work was supported by grants from Fundação de Amparo à Pesquisa do Estado de São Paulo (FAPESP; 2013/22733-0 and 2016/23008-5), Conselho Nacional de Desenvolvimento Científico e Tecnológico (CNPq; 473897/2011-3 and 444323/2014), and Coordenação de Aperfeiçoamento de Pessoal de Nível Superior (CAPES), as well as funding from National Institutes of Health (National Heart, Lung, and Blood Institute Grant 1R01HL129191.

DISCLOSURES

No conflicts of interest, financial or otherwise, are declared by the authors.

AUTHOR CONTRIBUTIONS

H.N.A., E.M., M.V.G., and L.R.S. conceived and designed research; H.N.A., T.I.L., D.S.P.S.F.G., A.G.O., B.C.F.-S., R.C.S.B., R.M.d.S.A., A.C., A.C.R., V.A.N., and L.R.S. performed experiments; H.N.A., D.S.P.S.F.G., A.G.O., B.C.F.-S., R.C.S.B., A.F.B.D., M.V.G., A.C.R., V.A.N., and L.R.S. analyzed data; H.N.A., D.S.P.S.F.G., A.G.O., M.V.G., A.C.R., V.A.N., and L.R.S. interpreted results of experiments; H.N.A. and L.R.S. prepared figures; H.N.A., V.A.N., and L.R.S. drafted manuscript; H.N.A., M.P.T.C.-M., E.M., M.V.G., E.M.C., A.C.R., V.A.N., and L.R.S. edited and revised manuscript; H.N.A., T.I.L., D.S.P.S.F.G., A.G.O., B.C.F.-S., R.C.S.B., A.F.B.D., A.C., M.P.T.C.-M., E.M., M.V.G., E.M.C., A.C.R., V.A.N., and L.R.S. approved final version of manuscript.

REFERENCES

1. **Anderson EJ, Lustig ME, Boyle KE, Woodlief TL, Kane DA, Lin CT, Price JW 3rd, Kang L, Rabinovitch PS, Szeto HH, Houmard JA, Cortright RN, Wasserman DH, Neufer PD.** Mitochondrial H_2O_2 emission and cellular redox state link excess fat intake to insulin resistance in both rodents and humans. *J Clin Invest* 119: 573–581, 2009. doi:10.1172/JCI37048.
2. **Barbosa MR, Sampaio IH, Teodoro BG, Sousa TA, Zoppi CC, Queiroz AL, Passos MA, Alberici LC, Teixeira FR, Manfiolli AO, Batista TM, Cappelli AP, Reis RI, Frasson D, Kettelhut IC, Parreiras-e-Silva LT, Costa-Neto CM, Carneiro EM, Curi R, Silveira LR.** Hydrogen peroxide production regulates the mitochondrial function in insulin resistant muscle cells: effect of catalase overexpression. *Biochim Biophys Acta* 1832: 1591–1604, 2013. doi:10.1016/j.bbadis.2013.04.029.
3. **Bartel DP.** MicroRNAs: target recognition and regulatory functions. *Cell* 136: 215–233, 2009. doi:10.1016/j.cell.2009.01.002.
4. **Boyerinas B, Park SM, Hau A, Murmann AE, Peter ME.** The role of let-7 in cell differentiation and cancer. *Endocr Relat Cancer* 17: F19–F36, 2010. doi:10.1677/ERC-09-0184.
5. **Castro A, Duft RG, Ferreira ML, Andrade AL, Gáspari AF, Silva LM, Oliveira-Nunes SG, Cavaglieri CR, Ghosh S, Bouchard C, Chacon-Mikahil MP.** Association of skeletal muscle and serum metabolites with maximum power output gains in response to continuous endurance or high-intensity interval training programs: the TIMES study—a randomized controlled trial. *PLoS One* 14: e0212115, 2019. doi:10.1371/journal.pone.0212115.
6. **Ebert MS, Sharp PA.** Roles for microRNAs in conferring robustness to biological processes. *Cell* 149: 515–524, 2012. doi:10.1016/j.cell.2012.04.005.
7. **Fan W, Waizenegger W, Lin CS, Sorrentino V, He MX, Wall CE, Li H, Liddle C, Yu RT, Atkins AR, Auwerx J, Downes M, Evans RM.** PPARδ promotes running endurance by preserving glucose. *Cell Metab* 25: 1186–1193.e4, 2017. doi:10.1016/j.cmet.2017.04.006.
8. **Fire A, Xu S, Montgomery MK, Kostas SA, Driver SE, Mello CC.** Potent and specific genetic interference by double-stranded RNA in *Caenorhabditis elegans*. *Nature* 391: 806–811, 1998. doi:10.1038/35888.
9. **Frost RJ, Olson EN.** Control of glucose homeostasis and insulin sensitivity by the *Let-7* family of microRNAs. *Proc Natl Acad Sci USA* 108: 21075–21080, 2011. doi:10.1073/pnas.1118922109.
10. **Giardine B, Riemer C, Hardison RC, Burhans R, Elnitski L, Shah P, Zhang Y, Blankenberg D, Albert I, Taylor J, Miller W, Kent WJ, Nekrutenko A.** Galaxy: a platform for interactive large-scale genome analysis. *Genome Res* 15: 1451–1455, 2005. doi:10.1101/gr.4086505.
11. **Heo I, Joo C, Cho J, Ha M, Han J, Kim VN.** Lin28 mediates the terminal uridylation of let-7 precursor MicroRNA. *Mol Cell* 32: 276–284, 2008. doi:10.1016/j.molcel.2008.09.014.
12. **Johnson SM, Grosshans H, Shingara J, Byrom M, Jarvis R, Cheng A, Labourier E, Reinert KL, Brown D, Slack FJ.** RAS is regulated by the let-7 microRNA family. *Cell* 120: 635–647, 2005. doi:10.1016/j.cell.2005.01.014.
13. **Jordan SD, Kriebs A, Vaughan M, Duglan D, Fan W, Henriksson E, Huber AL, Papp SJ, Nguyen M, Afetian M, Downes M, Yu RT, Kralli A, Evans RM, Lamia KA.** CRY1/2 selectively repress PPARδ and limit exercise capacity. *Cell Metab* 26: 243–255.e6, 2017. doi:10.1016/j.cmet.2017.06.002.
14. **Kelly DP, Scarpulla RC.** Transcriptional regulatory circuits controlling mitochondrial biogenesis and function. *Genes Dev* 18: 357–368, 2004. doi:10.1101/gad.1177604.
15. **Kurauti MA, Costa-Júnior JM, Ferreira SM, Dos Santos GJ, Protzek AO, Nardelli TR, de Rezende LF, Boschero AC.** Acute exercise restores insulin clearance in diet-induced obese mice. *J Endocrinol* 229: 221–232, 2016. doi:10.1530/JOE-15-0483.

16. **Langmead B, Trapnell C, Pop M, Salzberg SL.** Ultrafast and memory-efficient alignment of short DNA sequences to the human genome. *Genome Biol* 10: R25, 2009. doi:10.1186/gb-2009-10-3-r25.
17. **Lee YS, Dutta A.** The tumor suppressor microRNA *let-7* represses the HMGA2 oncogene. *Genes Dev* 21: 1025–1030, 2007. doi:10.1101/gad.1540407.
18. **Lin J, Wu H, Tarr PT, Zhang CY, Wu Z, Boss O, Michael LF, Puigserver P, Isotani E, Olson EN, Lowell BB, Bassel-Duby R, Spiegelman BM.** Transcriptional co-activator PGC-1α drives the formation of slow-twitch muscle fibres. *Nature* 418: 797–801, 2002. doi:10.1038/nature00904.
19. **Liu Z, Butow RA.** Mitochondrial retrograde signaling. *Annu Rev Genet* 40: 159–185, 2006. doi:10.1146/annurev.genet.40.110405.090613.
20. **Livak KJ, Schmittgen TD.** Analysis of relative gene expression data using real-time quantitative PCR and the $2^{-\Delta\Delta CT}$ method. *Methods* 25: 402–408, 2001. doi:10.1006/meth.2001.1262.
21. **Murchison EP, Partridge JF, Tam OH, Cheloufi S, Hannon GJ.** Characterization of Dicer-deficient murine embryonic stem cells. *Proc Natl Acad Sci USA* 102: 12135–12140, 2005. doi:10.1073/pnas.0505479102.
22. **Narkar VA, Downes M, Yu RT, Embler E, Wang YX, Banayo E, Mihaylova MM, Nelson MC, Zou Y, Juguilon H, Kang H, Shaw RJ, Evans RM.** AMPK and PPARδ agonists are exercise mimetics. *Cell* 134: 405–415, 2008. doi:10.1016/j.cell.2008.06.051.
23. **Perez-Schindler J, Philp A.** Regulation of skeletal muscle mitochondrial function by nuclear receptors: implications for health and disease. *Clin Sci (Lond)* 129: 589–599, 2015. doi:10.1042/CS20150246.
24. **Pérez-Schindler J, Summermatter S, Salatino S, Zorzato F, Beer M, Balwierz PJ, van Nimwegen E, Feige JN, Auwerx J, Handschin C.** The corepressor NCoR1 antagonizes PGC-1α and estrogen-related receptor α in the regulation of skeletal muscle function and oxidative metabolism. *Mol Cell Biol* 32: 4913–4924, 2012. doi:10.1128/MCB.00877-12.
25. **Puigserver P, Spiegelman BM.** Peroxisome proliferator-activated receptor-γ coactivator 1α (PGC-1α): transcriptional coactivator and metabolic regulator. *Endocr Rev* 24: 78–90, 2003. doi:10.1210/er.2002-0012.
26. **Puigserver P, Wu Z, Park CW, Graves R, Wright M, Spiegelman BM.** A cold-inducible coactivator of nuclear receptors linked to adaptive thermogenesis. *Cell* 92: 829–839, 1998. doi:10.1016/S0092-8674(00)81410-5.
27. **Reinhart BJ, Slack FJ, Basson M, Pasquinelli AE, Bettinger JC, Rougvie AE, Horvitz HR, Ruvkun G.** The 21-nucleotide *let-7* RNA regulates developmental timing in *Caenorhabditis elegans*. *Nature* 403: 901–906, 2000. doi:10.1038/35002607.
28. **Rottiers V, Najafi-Shoushtari SH, Kristo F, Gurumurthy S, Zhong L, Li Y, Cohen DE, Gerszten RE, Bardeesy N, Mostoslavsky R, Näär AM.** MicroRNAs in metabolism and metabolic diseases. *Cold Spring Harb Symp Quant Biol* 76: 225–233, 2011. doi:10.1101/sqb.2011.76.011049.
29. **Safdar A, Abadi A, Akhtar M, Hettinga BP, Tarnopolsky MA.** miRNA in the regulation of skeletal muscle adaptation to acute endurance exercise in C57Bl/6J male mice. *PLoS One* 4: e5610, 2009. doi:10.1371/journal.pone.0005610.
30. **Savage DB, Petersen KF, Shulman GI.** Disordered lipid metabolism and the pathogenesis of insulin resistance. *Physiol Rev* 87: 507–520, 2007. doi:10.1152/physrev.00024.2006.
31. **Scarpulla RC.** Transcriptional paradigms in mammalian mitochondrial biogenesis and function. *Physiol Rev* 88: 611–638, 2008. doi:10.1152/physrev.00025.2007.
32. **Shanely RA, Zwetsloot KA, Triplett NT, Meaney MP, Farris GE, Nieman DC.** Human skeletal muscle biopsy procedures using the modified Bergström technique. *J Vis Exp* 91: e51812, 2014. doi:10.3791/51812.
33. **Sprecher DL, Massien C, Pearce G, Billin AN, Perlstein I, Willson TM, Hassall DG, Ancellin N, Patterson SD, Lobe DC, Johnson TG.** Triglyceride:high-density lipoprotein cholesterol effects in healthy subjects administered a peroxisome proliferator activated receptor δ agonist. *Arterioscler Thromb Vasc Biol* 27: 359–365, 2007. doi:10.1161/01.ATV.0000252790.70572.0c.
34. **Wu Z, Puigserver P, Andersson U, Zhang C, Adelmant G, Mootha V, Troy A, Cinti S, Lowell B, Scarpulla RC, Spiegelman BM.** Mechanisms controlling mitochondrial biogenesis and respiration through the thermogenic coactivator PGC-1. *Cell* 98: 115–124, 1999. doi:10.1016/S0092-8674(00)80611-X.
35. **Yamamoto H, Williams EG, Mouchiroud L, Cantó C, Fan W, Downes M, Héligon C, Barish GD, Desvergne B, Evans RM, Schoonjans K, Auwerx J.** NCoR1 is a conserved physiological modulator of muscle mass and oxidative function. *Cell* 147: 827–839, 2011. doi:10.1016/j.cell.2011.10.017.
36. **Zhu H, Shah S, Shyh-Chang N, Shinoda G, Einhorn WS, Viswanathan SR, Takeuchi A, Grasemann C, Rinn JL, Lopez MF, Hirschhorn JN, Palmert MR, Daley GQ.** *Lin28a* transgenic mice manifest size and puberty phenotypes identified in human genetic association studies. *Nat Genet* 42: 626–630, 2010. doi:10.1038/ng.593.
37. **Zhu H, Shyh-Chang N, Segrè AV, Shinoda G, Shah SP, Einhorn WS, Takeuchi A, Engreitz JM, Hagan JP, Kharas MG, Urbach A, Thornton JE, Triboulet R, Gregory RI, Altshuler D, Daley GQ; DIAGRAM Consortium; MAGIC Investigators.** The *Lin28/let-7* axis regulates glucose metabolism. *Cell* 147: 81–94, 2011. doi:10.1016/j.cell.2011.08.033.